Phys. Status Solidi B **252,** No. 10, 2230–2235 (2015) / **DOI** 10.1002/pssb.201552129

physica status solidi b
www.pss-b.com
basic solid state physics

Interpolating the optical properties of varied composition silicon nitride

Andrew Thomson*, **Niraj Lal, and Yimao Wan**

The Research School of Engineering, The Australian National University, Canberra 0200, Australia

Received 4 March 2015, revised 4 June 2015, accepted 9 June 2015
Published online 10 July 2015

Keywords solar cells, silicon nitride, optical properties, tetrahaedron

* Corresponding author: e-mail andrew.thomson@anu.edu.au, Phone: +61-2-61258297, Fax: +61-2-612588820

We develop a method for interpolating the optical properties of silicon nitride formed with different deposition parameters. Published refractive index measurements for eight silicon nitride films formed by in-line microwave plasma-enhanced chemical-vapour deposition with a range of ammonia to silane gas-flow ratios are modelled and interpolated. The measurements are fitted by a physical model for the optical properties of silicon nitride. The model considers 16 different silicon-centred, silicon, nitrogen, hydrogen tetrahedron bond configurations in an effective medium with vacuum. An average root mean squared error (RMSE) of 0.36, was calculated when using the physical model, which is high when compared to a simple semi-physical model which achieves an average RMSE of 0.06. The semi-physical model is similar to the tetrahedron model. However, the scale and shifts variables are used as fit parameters compared to being calculated for a physical tetrahedron configuration. The poor fitting of the tetrahedron model empirically suggests that additional bond arrangements need be considered, in particular tetrahedra with vacant bonds. Our global interpolation over the optical properties measured for multiple films mitigates measurement and modelling error. It leads to a smooth optical function with changing gas ratio which aides in optimisation of multi-layer and graded anti-reflection coatings.

1 Introduction Silicon nitride (SiN_x) is a typical anti-reflection coating (ARC) on silicon solar cells. The extensive use of SiN_x as an ARC are due to its optical properties and its passivating effects on silicon surfaces and bulk defects [1–4]. The impact of SiN_x on crystalline silicon (c-Si) varies significantly with composition and deposition method [5]. SiN_x deposited by plasma-enhanced chemical-vapour deposition (PECVD) is an amorphous material, with tuneable refractive index N and dielectric constant ϵ ($\epsilon = N$) adjusted by altering the SiN_x composition [5–9]. The real component of the N at wavelength λ at 633 nm $n_{633\,nm}$ can be readily varied continuously from 1.8 to 3.2 by altering the deposition conditions [5, 7, 8]. Characterisation of such a variable material poses significant challenges when producing c-Si solar cells and microelectronic devices.

We investigate methods for modelling and interpolating the optical properties of SiN_x deposited by in-line microwave PECVD. We model the optical data from Duttagupta et al. [7], reproduced in Fig. 1, hereafter referred to as the target optical data. The N of the target optical data was varied by altering the deposition gas-flow ratios—the ratio of the flow rate of ammonia to silane (NH_3:SiH_4) deposition gasses, varying the composition of reactants for film formation.

The target optical data is representative of films used in the production of c-Si solar cells and is used by the solar cell modelling software OPAL2 [10]. Practical interpolation of the target optical data enables the optimisation of both film thickness and refractive index. We note that the modelling and interpolation process can be applied to other data sets [5, 9, 11].

In this paper, we

(i) Propose a variant on an established optical model of SiN_x films [12–14]. Our modelling performs as well as the commonly used Tauc–Lorentz (TL) model [15, 16] achieving equivalent root mean square error (RMSE). Further, the fitting of the target optical data with our model requires three fit parameters compared to five for the TL model.
(ii) Use our SiN_x optical model to interpolate the target optical data by performing regressions of the model parameters, giving a smooth function for N which

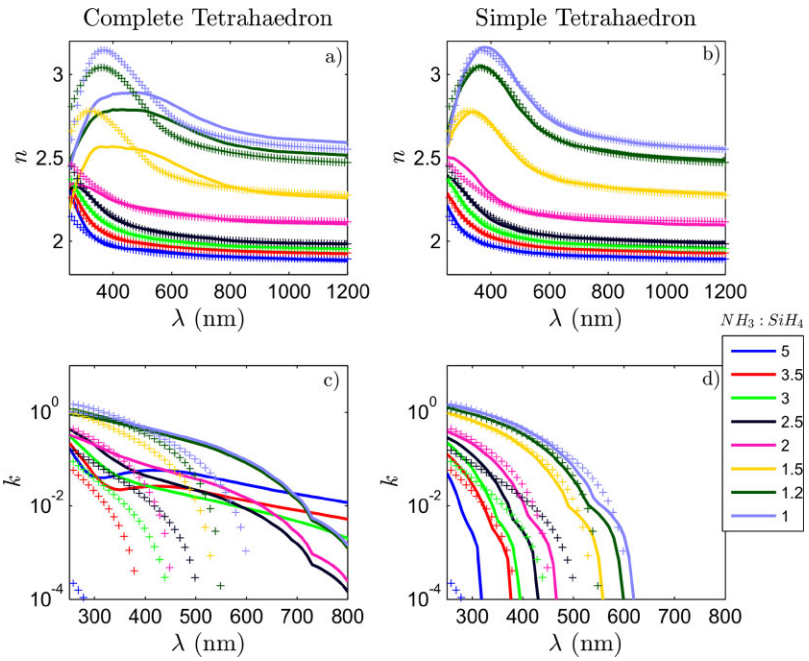

Figure 1 Modelled and measured n and k plotted versus λ for SiN_x films with varying flow ratios. We depict the target optical data by the + markers from Ref. [7]. Overlaid on the target optical data are the fits of the complete-tetrahedron model (plots (a) and (c)) and the simple-tetrahedron model (plots (b) and (d)). Both fits are represented by the solid lines.

depends on wavelength λ and flow ratio, within the ranges of that used to generate the target optical data.

(iii) Use the optical model to demonstrate the impact of flow ratio and film thickness t_{arc} on current generated in a c-Si solar cell in air and encapsulated in ethylene-vinyl acetate (EVA) and glass. The optimums for $n_{633\,nm}$ are 1.90 and 2.18 and t_{arc} are 79.4 and 70.4 nm for cells in air and encapsulated, respectively.

We compare two approaches for modelling the target optical data. The first, a physical model based on the optical properties of silicon-centred tetrahedra [12–14, 17]. Referred to as the complete-tetrahedron model. The complete-tetrahedron model combines the dielectric function for 16 Si, N and H tetrahedron bonding configurations ($Si_xN_yH_z$). The second is a semi-physical model, which is similar to the complete-tetrahedron model. The semi-physical model, referred to as the simple-tetrahedron model, shifts and scales the dielectric function of amorphous silicon (a-Si) in combination with the dielectric function of low-pressure CVD-deposited stoichiometric silicon nitride Si_3N_4.

We make two observations:

(i) The complete-tetrahedron model cannot accurately model the target optical data for films with an $n_{633\,nm}$ greater than 2.15. Fitting the high-index measurements results in an RMSE that is 3–10 times larger than the TL model.

(ii) The simple-tetrahedron model provides a good fit to the target data, with an average RMSE ($RMSE_g = 0.06$) equivalent to the TL model ($RMSE_g = 0.07$).

Importantly, the simple-tetrahedron model affords excellent fits to a range of SiN_x films. When modelling a series of measurements, such as the target optical data, it provides a practical method for predicting the optical properties of films with intermediate composition, discussed further below and exhibited in Fig. 4.

The outline of this paper is as follows. First, methodology for modelling the target optical data. Second, results of the fitting both the complete- and the simple-tetrahedron model to the target optical data. Third, discussion of the implications for tetrahedra modelling of SiN_x composition layers and concluding statements on the paper are made.

2 Method and calculation In this section, we describe the methods for the modelling the N of SiN_x target data. The complex dielectric function of a material ε is equivalent to the square of the N

$$\tilde{\epsilon} = \tilde{N}^2, \quad \text{where} \quad \tilde{\epsilon} = \varepsilon_1 + i\varepsilon_2 \quad \text{and} \quad \tilde{N} = n + ik. \tag{1}$$

We employ the root-mean-squared error, defined for the j^{th} measurement of the target data

$$\mathrm{RMSE}_j = \sqrt{\frac{\sum_{i=1}^{P} \left(\epsilon_{\mathrm{target}}(\lambda(i)) - \epsilon_{\mathrm{model}}(\lambda(i))\right)^2}{P}} \tag{2}$$

which represents the effectiveness of the modelling technique. In this case $\epsilon_{t\,arget}$ is the discrete measured data and is given at P discrete wavelengths, ϵ_{model} is the model's predicted dielectric function, evaluated at the same λ. To assess the accuracy of the modelling technique to fit the

target data the average $RMSE_j$ is taken, giving the global $RMSE_g$ denoted by the subscript g.

Spectroscopic ellipsometry (SE) measurements of thin-SiN_x films on silicon formed by the in-line microwave PECVD, generated the target optical data. SE measures the ratio of the reflected s and p polarizations as a function of λ

$$\rho(\lambda) = \frac{r_p(\lambda)}{r_s(\lambda)} = \tan(\Psi(\lambda))e^{i\Delta(\lambda)} \tag{3}$$

where the Ψ and Δ response were replicated by modelling the physical system. Typically the fitting of Ψ and Δ is achieved by performing transfer-matrix-method calculations [18] for an optical stack with a generalised material represented by the TL optical model atop of silicon. As described by Jellison and Modine [15, 16], the TL model has five fit parameters in order to replicate the $\Psi(\lambda)$ and $\Delta(\lambda)$ responses. The TL model combines the Tauc absorption expression for energies above the bandgap [19]. With the Lorentz model of absorption that represents non-interacting atoms with electron electromagnetic wave interaction [20]. The combination of these models gives a four parameter expression for ε_2. In this case Kramers–Kronig (KK) integration [21] is applied to ε_2 yielding ε_1, with an additional parameter ε_1 (∞). The expressions for ε_1 and ε_2 by the TL model are in Refs. [15, 16].

We refit the TL model n and k to the target optical data [7], to ascertain the minimum attainable error. If we employ the same fitting algorithm and initial conditions, the RMSE should be zero. We replicate the target optical data with little error (RMSE = 0.07). Discretisation is equivalent to a 0.01 RMSE contribution we assume differences in the modelling procedure including the initial conditions, which the authors did not report [7], are responsible for the remainder of the error.

2.1 The complete-tetrahedron model The dielectric function of 16 silicon-centred tetrahedra were combined to fit the target optical data with a physical-material model [12, 13]. To merge the impact of multiple species of tetrahedron on the optical properties of SiN_x Bruggemann EMA [22] is applied which infers

$$\sum_{m=1}^{M} v_m \frac{\epsilon_m - \epsilon}{\epsilon_m + 2\epsilon} = 0 \tag{4}$$

where ϵ_m is the dielectric function and v_m is the total fraction of the m^{th} tetrahedron, respectively. The total fraction sums to 1:

$$\sum_{m=1}^{M} v_m = 1. \tag{5}$$

The dielectric function of distinct tetrahedra is not measurable, as it is impractical to fabricate homogeneous material of individual tetrahedra. The exceptions are the materials a-Si and Si_3N_4 [14]. Aspenes and Theeten developed a method to estimate tetrahedra bond configuration. The process scales and shifts the dielectric function of the measurable reference materials a-Si and Si_3N_4 [14]. Aspenes and Theeten describe the tetrahedra dielectric function as

$$\tilde{\epsilon}_m(E) = 1 + c_{1,m}(\tilde{\epsilon}_{\text{ref}}(c_{2,m}) - 1) \tag{6}$$

where c_1 and c_2 are the scale and shift parameters. In this work we use c_1 and c_2 calculated by Yin and Smith for the physical tetrahedra arrangements listed in Table 1 [12, 13]. Table 1 summarises the tetrahedron, scaling parameters and reference dielectric measurements, measured by Phillipp [23, 24], used to model the optical data in Fig. 1.

In order to generate $\tilde{\epsilon}_{\text{model}}$ Eq. (4) was solved using the $\tilde{\epsilon}_m$ from Eq. (6) for the 16 bonding configurations listed in Table 1, with the inclusion of voids with the dielectric function $\tilde{\epsilon}_{\text{void}} = 1 + 0i$ for all λ, at a fraction v_i in accordance with Eq. (5). The fraction of each bonding components v_i were used as free parameters to model the target optical data. To fit the data both non-linear least squares and genetic algorithms where employed in MatLab to best fit the data.

2.2 The simple-tetrahedron model A simple shifting and scaling model is developed analogous to Aspenes and Theeten [14], where they demonstrated that the $\tilde{\epsilon}$ of amorphous silicon a-Si could be used to predict the $\tilde{\epsilon}$ of Si_3N_4 using Eq. (6) with the scaling factors $c_1 = 0.32$ and $c_2 = 0.37$. The $\tilde{\epsilon}$ of a-Si and Si_3N_4 was measured by Philipp [23, 24]. Instead of computing c_1 and c_2 based on the physical properties of tetrahedral configurations, we use them as fit parameters. We use c_1 and c_2 to shift and scale ε_{ref}(taken to be a-Si), giving ε by Eq. (6). We further

Table 1 List of the tetrahedron scaling parameters and reference dielectric function taken from Tables 1, 2 and 3 of Ref. [13]. We list the $n_{633\,\text{nm}}$ calculated from Eq. (6).

tetrahedron	c_1	c_2	$\tilde{\varepsilon}_{\text{ref}}$	$n_{633\,\text{nm}}$
Si-Si_4	1	1	a-Si	4.26
Si-Si_3N	0.824	0.832	a-Si	4.14
Si-Si_2N_2	0.610	0.671	a-Si	3.13
Si-SiN_3	0.413	0.523	a-Si	1.30
Si-N_4	0.257	0.395	a-Si	0.70
Si-N_4	1	1	Si_3N_4	2.02
Si-N_3(NH)	0.846	0.949	Si_3N_4	1.91
Si-N_2(NH)$_2$	0.745	0.912	Si_3N_4	1.84
Si-N_1(NH)$_3$	0.677	0.886	Si_3N_4	1.79
Si-(NH)$_4$	0.630	0.867	Si_3N_4	1.75
Si-HN(HN)$_2$	0.826	0.912	Si_3N_4	1.89
Si-HN_2(HN)	0.908	0.926	Si_3N_4	1.95
Si-Si(HN)$_3$	1.171	1.196	Si_3N_4	2.13
Si-SiN(HN)$_2$	1.274	1.227	Si_3N_4	2.20
Si-SiN_2(HN)	1.428	1.271	Si_3N_4	2.30
Si-Si_2N_2	2.539	1.714	Si_3N_4	2.92

assume the material as an effective medium of two components, fraction v_1 arises from the scaled and shifted ε of a-Si, the second component $f_{Si_3N_4} = 1 - v_1$ is Si_3N_4. To minimise $RMSE_j$, c_1, c_2 and $f_{Si_3N_4}$ are varied for each of the target optical data measurements. Both non-linear least squares and genetic algorithms were employed to fit the data.

3 Results We plot the results of fitting the complete- and simple-tetrahedron models to the target optical data in Fig. 1a and c and Fig. 1b and d, respectively. The solid lines depict the modelled n and k, and the + coloured markers depict the target optical data.

The complete-tetrahedron model fits the low refractive index films ($n_{633nm} \leq 2.15$) well with RMSE < 0.1. When observing the complete-tetrahedra data compared to target optical data we see the tetrahedra determined by Yin and Smith do not provide a good fit. There are significant discrepancies in k for $\lambda > 500$ nm, and in n for $\lambda < 500$ nm for the high-index material ($n_{633\,nm} > 2.15$). The simple-tetrahedron model provides a good fit to the target optical data $RMSE_g = 0.06$ compared to $RMSE_g = 0.07$ for the TL model, fitting all eight measurements well replicating both the n and k.

To quantitatively compare the fits, Fig. 2 plots the RMSE as a function of $n_{633\,nm}$, scaled to the deposition flow ratio, for the associated fitted data for each modelling method. Included is the fit of the TL model—an indication of the lowest expected error. Both the fitting of the complete and simple models perform well for low-index films ($n_{633\,nm} \leq 2.15$). However, we see the complete-tetrahedron model does not sufficiently capture the physics of the dielectric constants of high-index materials as is indicated by Fig. 1 plot c. Finally, we summarise the $RMSE_g$ for all approaches in Table 2 along with the number parameters per fit and the total parameters for all eight fits to the target optical data. Included in Table 2 are the entries for the regression of the simple-tetrahedron model which we detail in the discussion.

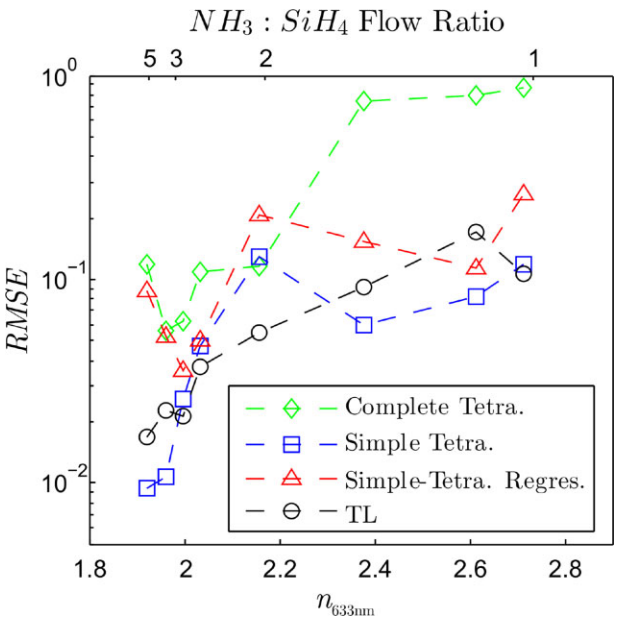

Figure 2 RMSE as a function of n_{633nm} for model fits to the target optical data. The error was computed by Eq. (1) for four methods: the simple- and complete-tetrahedron models, the regression of the simple-tetrahedron model and the fit of the TL model.

The simple-tetrahedron model shows a good fit to the target optical data, reproducing the data modelled by the TL and demonstrating the three-parameter model can model a range of SiN_x films. To aid in the interpolation of target optical data, we plot the fitted parameters c_1, c_2 and $f_{Si_3N_4}$ versus $n_{633\,nm}$ of the target optical data scaled to the flow ratio in Fig. 3. The trends in the parameters are fitted well by a decaying exponential and two regression lines, respectively. Where the seven regressions parameters—four for both the linear regressions and three for the exponential decay regression—can represent an optical model that interpolates all of the optical data. The $RMSE_g$ is included in Table 2, it is considerably higher than the simple-tetrahedron model, but better than the complete-tetrahedron model.

To demonstrate the interpolation of the simple-tetrahedron model, we predict the optical properties of films with intermediate composition, which can routinely be generated by altering the gas flows of ammonia and silane. A contour plot of the optical properties is given in Fig. 4 as a function of $n_{633\,nm}$ and scaled to the reported flow ratio. The surface was produced by utilising the regressions of the data in Fig. 3 evaluated at λ from 200–1200 nm, relevant to silicon solar cells.

4 Discussion and conclusion In this study, we find the complete-tetrahedron model does not match the target optical data. As the complete-tetrahedral model considers the bonding configuration determined by Yin and Smith [12, 13]. We suggest the discrepancy is due to the presence of hydrogenated silicon nitride tetrahedra not previously considered or indeed tetrahedra with a vacancy. Studies

Table 2 Summary of the average RMSE for the fits of the simple- and complete-tetrahedron models to the target optical data. Also, included is the regression fit of the simple-tetrahedron model described in the discussion. For comparison, the TL fit is include giving an indication of the minimum error. We list the number of parameters for each method for both the individual fit, and the total number of parameters to describe the modelling of all eight measurements of the target optical data.

	parameters		
fitting method	per fit	total	$RMSE_g$
complete-tetrahedra	16	134	0.36
simple-tetrahedra	3	48	0.06
simple-tetra. regres.	n/a	7	0.12
TL refit.	5	80	0.07

have shown that vacancies in SiN_x create *K*-centres [25, 26] —a defect that can have its charge state altered. Charge modification of *K*-centres is an effect exploited in the fabrication of solid-state memory [27] and the passivation of solar cells [28]. The scaling of the optical properties of a-Si can achieve excellent fits to the target optical data where c_1 and c_2 are varied freely, exhibited by the simple-tetrahedron model. While our fitting results are not proof that additional tetrahedra dominate the optical properties of silicon-rich films, they empirically suggest that the tetrahedra modelling could be extended.

The simple-tetrahedron model was fitted to all eight optical measurements. By performing a regression of the three model parameters, as seen in Fig. 3, we create an optical model for SiN_x that globally interpolates all of the films. The surfaces in Fig. 4a and b have a smoothing effect on the optical parameters, compared to the piecewise linear interpolations that were implemented by Nagel et al. in their optimisation directly of the $\tilde{N}$ data [9]. Assuming the optical properties of SiN_x vary continuously with varying stoichiometry, as is the case with the Bruggemann EMA [22]. The smoothing from the regression mitigates errors in the individual optical measurements and fits. Hence a global fit to multiple films of varied stoichiometry may better reflect the underlying impact of the physical changes in the films on the optics. Confirmation of this assertion requires detailed study.

Nevertheless, the smooth optical function is useful for optimisation, for ARC, stack ARC and indeed graded ARC [29, 30]. Indeed if using the parameters appended in Table 3, following the procedure outlined in Ref. [10] for determination of J_{gen}. The calculations accounted for planar cells in air and encapsulated in 3.2 mm glass a 400 μm of EVA. We observed the clear optimums in J_{gen} for $n_{633\,nm}$ of 1.90 and 2.18 with thicknesses of 79.4 and 70.4 nm, for a cell in air and EVA and glass, respectively. The calculated optimums of 36.5 and 34.9 mA/cm^2 are similar to those calculated by Nagel et al. [9]. These calculations employed the optical model represented in Fig. 4, computed from the regression of the fit parameters in Fig. 3.

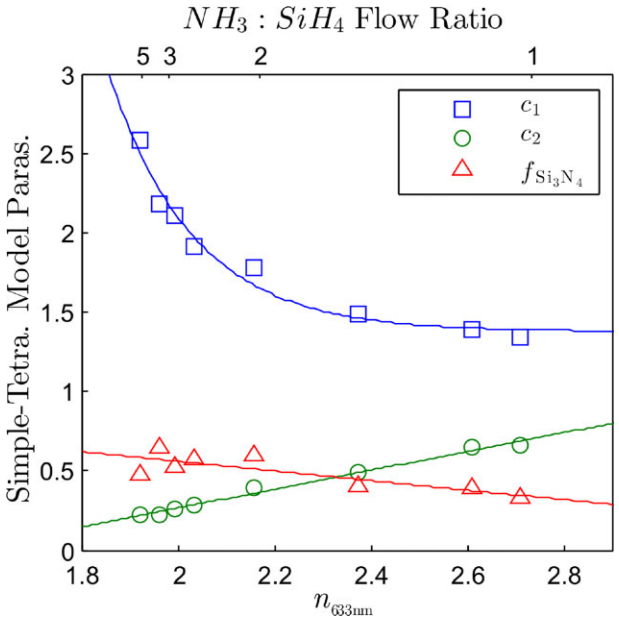

Figure 3 Plot of the simple-tetrahedron model's parameters resulting from non-linear optimisation to the target optical data. The lines are regressions, linear for c_2 and $f_{Si_3N_4}$, and a single-order exponential decay for c_1. The regression parameters are used to generate the surface in Fig. 4.

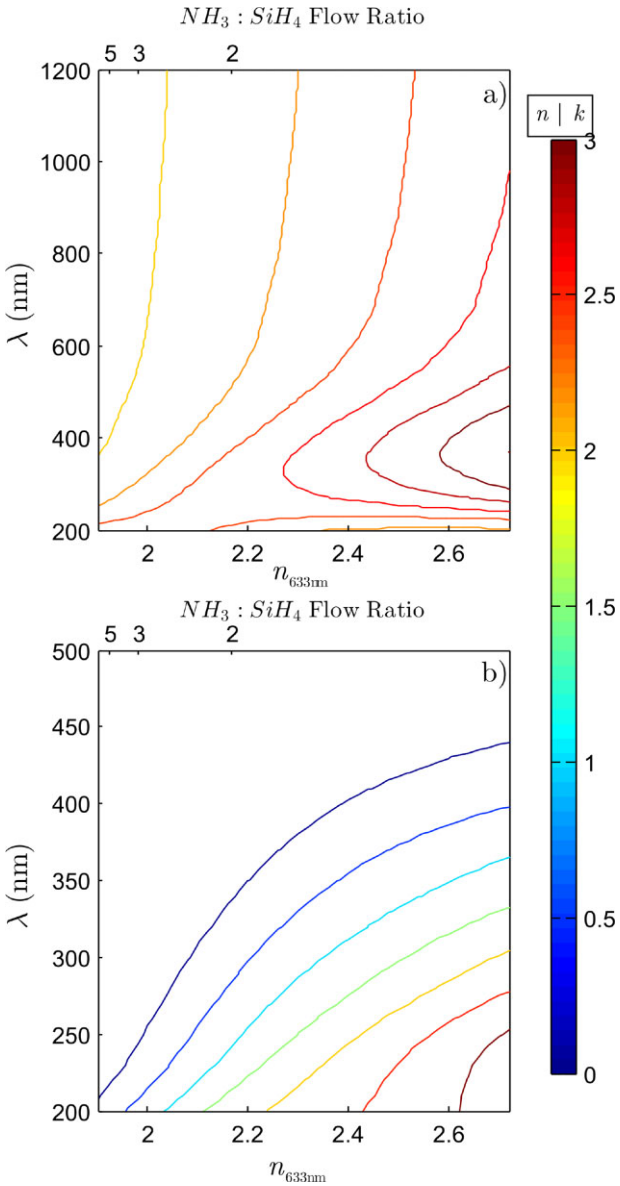

Figure 4 Refractive index contour plots for SiN_x generated by globally fitting the optical properties of SiN_x films produced by Duttaguptta *et al.* [7], formed by using the regressions to the parameters in Fig. 3.

Table 3 Cell J_{sc} modelling details.

name	parameter	source
simulation	planar 1d	–
calculation	transfer matrix	[18]
spectrum	AM1.5 g	
air	$\tilde{N} = 1 + i0$	
glass	3.2 mm Starphire	[31]
encapsulant	400 μm EVA	[31]
Si	Green	[32]
path length Z	360 μm	double pass 180 μm cell
J_{gen}		[10]
IQE	1 for all λ	[10]

In conclusion, we have developed and tested a method for fitting the optical properties of varied composition SiN_x films and compared it to the tetrahedron and TL optical models. The simple-tetrahedron model has one-quarter of the RMSE of the tetrahedron physical model and comparable error to a free TL model for the target optical data. We suggest this modelling technique, or variants of it are applied to other SiN_x data sets. Ultimately improved modelling of SiN_x optics, formed via a range of deposition methods, will lead to an enhanced understanding of the materials and device optimisation, including the development of graded and multi-layer ARC.

Acknowledgments The authors would like to acknowledge the support of the Australian Renewable Energy Agency in the funding of this work through grant 3-F006. We would also like to thank Ziv Hameiri, Tom White and Malte Vogt for their advice and helpful discussions on this work.

References

[1] H. Nagel, J. Schmidt, A. Arberle, and R. Hezel, "Exceptionally high bulk minority-carrier lifetimes in block-cast multicrystalline silicon," presented at the 14th European Photovoltaic Solar Energy Conference, Barcelona, Spain, 1997.
[2] T. Lauinger, J. Schmidt, A. G. Aberle, and R. Hezel, Appl. Phys. Lett. **68**, 1232–1234 (1996).
[3] F. Duerinckx and J. Szlufcik, Sol. Energy Mater. Sol. Cells **72**, 231–246 (2002).
[4] A. G. Aberle, Sol. Energy Mater. Sol. Cells **65**, 239–248 (2001).
[5] Y. Wan, K. R. McIntosh, and A. F. Thomson, AIP Adv. **3**, 032113 (2013).
[6] S. Winderbaum, I. G. Romijn, D. Sterk, and B. van Straaten, "MW PECVD a-Si_xNYHZ: the road to optimum silicon nitride coatings," presented at the 21st European Photovoltaic Solar Energy Conference, Dresden, Germany, 2006.
[7] S. Duttagupta, F. Ma, B. Hoex, T. Mueller, and A. G. Aberle, Energy Proc. **15**, 78–83 (2012).
[8] T. Lauinger, J. Moschner, A. G. Aberle, and R. Hezel, J. Vac. Sci. Technol. A **16**, 530–543 (1998).
[9] H. Nagel, A. G. Aberle, and R. Hezel, Prog. Photovolt. **7**, 245–260 (1999).
[10] K. R. McIntosh and S. C. Baker-Finch, in: 2012 38th IEEE Photovoltaic Specialists Conference (PVSC), Austin, USA, 2012, pp. 000265–000271.
[11] J. F. Lelièvre, J. De la Torre, A. Kaminski, G. Bremond, M. Lemiti, R. El Bouayadi, et al., Thin Solid Films **511–512**, 103–107 (2006).
[12] Z. Yin and F. W. Smith, Phys. Rev. B **42**, 3666–3675 (1990).
[13] Z. Yin and F. W. Smith, Phys. Rev. B **42**, 3658–3665 (1990).
[14] D. E. Aspnes and J. B. Theeten, J. Appl. Phys. **50**, 4928–4935 (1979).
[15] G. E. Jellison, Jr., and F. A. Modine, Appl. Phys. Lett. **69**, 371–373 (1996).
[16] G. E. Jellison and F. A. Modine, Appl. Phys. Lett. **69**, 2137–2137 (1996).
[17] A. Sassella, Phys. Rev. B **48**, 14208–14215 (1993).
[18] H. A. Macleod, "Basic Theory," in: Thin-Film Optical Filters, 3rd edn. (CRC Press, Taylor and Francis Group, Boca Raton, Florida, USA, 2001), pp. 12–85.
[19] J. Tauc, R. Grigorovici, and A. Vancu, Phys. Status Solidi B **15**, 627–637 (1966).
[20] F. Wooten, Optical Properties of Solids (Academic Press, New York, 1972), pp. 42–52.
[21] P. C. Martin, Phys. Rev. **161**, 143–155 (1967).
[22] D. A. G. Bruggeman, Ann. Phys. (Leipzig) **416**, 636–664 (1935).
[23] H. R. Philipp, J. Electrochem. Soc. **120**, 295–300 (1973).
[24] H. R. Philipp, J. Phys. Chem. Solids **32**, 1935–1945 (1971).
[25] W. L. Warren, J. Robertson, and J. Kanicki, Appl. Phys. Lett. **63**, 2685–2687 (1993).
[26] W. L. Warren, P. M. Lenahan, and S. E. Curry, Phys. Rev. Lett. **65**, 207–210 (1990).
[27] M. H. White, Y. Yang, P. Ansha, and M. L. French, IEEE Trans. Compon. Packag. Manuf. Technol. A **20**, 190–195 (1997).
[28] K. J. Weber and H. Jin, Appl. Phys. Lett. **94**, 063509 (2009).
[29] K.-H. Kim and Q.-H. Park, Sci. Rep. **3**, 1062 (2013).
[30] A. Mahdjoub and L. Zighed, Thin Solid Films **478**, 299–304 (2005).
[31] K. R. McIntosh, J. N. Cotsell, J. S. Cumpston, A. W. Norris, N. E. Powell, and B. M. Ketola, in: 2009 34th IEEE Photovoltaic Specialists Conference (PVSC), Philadelphia, USA, 2009, pp. 000544–000549.
[32] M. A. Green, Sol. Energy Mater. Sol. Cells **92**, 1305–1310 (2008).